

Petri net based modelling and simulation of p16-Cdk4/6-Rb pathway

Nimet İlke Çetin,¹ Rza Bashirov,¹ Şükrü Tüzmen²

¹ Department of Applied Mathematics and Computer Science

² Department of Biological Sciences,

Eastern Mediterranean University, Famagusta, North Cyprus, Mersin-10, Turkey

{ilke.cetin;rza.bashirov;sukru.tuzmen}@emu.edu.tr

Abstract. Tumor suppressor gene p16 is of utmost interest in investigation of signal transduction pathways due to its gatekeeper role at the G1/S checkpoint of the cell cycle. Defects in p16 result in uncontrolled cell division which leads to progression of malignancy in an organism. In the present research we focus on p16-Cdk4/6-Rb pathway which is a cornerstone of G1 phase of the cell cycle. We implement Pet net formalism and Cell Illustrator software tool to create model of p16-Cdk4/6-Rb pathway and perform a series of simulations to validate the model.

Keywords: Replicative senescence, Cell cycle, p16-Cdk4/6-Rb pathway, Hybrid functional Petri net, Cell Illustrator

1 Introduction

1.1 Biological context

Cell division is a fundamental biological process that is essential to continuity of all living organisms. Cell replication or growth is controlled by a complex network of signals, that control the cell cycle. During the cell cycle cells grow to twice their size, copy their chromosomes, and divide into two new cells. The cell cycle is composed of four distinct phases: G1-phase (gap 1), S-phase (synthesis), G2-phase (gap 2) and M-phase (mythosis) [14]. Cell cycle checkpoints are used between neighboring phases to monitor and regulate the progress of the cell cycle. A cell cannot proceed to the next phase until otherwise checkpoint requirements have been met.

Tumor suppressor gene p16 plays important role in regulating cell grows and division at checkpoint G1/S [34]. The p16 gene is major tumor suppressor gene that is responsible for replicative senescence. Cell division is not an infinitely continuous process as cells undergo a finite number of cumulative population doublings [17]. Most human normal cells permanently stop dividing after a 50-75 cell divisions and enter a state termed cellular or replicative senescence [17]. Most tumors contain cells that appear to have bypassed this limit and evaded replicative senescence. Immortality, or even an extended replicative lifespan, greatly increases susceptibility to malignant progression because it permits

the extensive cell divisions needed to acquire successive mutations. Thus, cellular senescence may act as a barrier to cancer and play an important role in tumor suppression [8]. Inactivation of tumor suppressor gene p16, which in fact keeps track of replicative senescence, results in uncontrolled cell division, which leads to cancer [4].

During G1 phase, proteins Cdk4 and Cdk6 form complex with protein CycD, which in turn phosphorylates the Rb protein family. When Rb is phosphorylated by Cdk4/6 it loses its function and releases its target, the E2F family transcription factors, resulting in the initiation of DNA replication [31, 32]. Otherwise Rb inhibits transcription factor E2F [36]. E2F is a transcription factor which initiates transcription of genes required for S phase [5]. In the case of malignant progression action of p16 inhibits binding of Cdk4/6 with CycD which leaves Rb, and other Rb related proteins [25, 35]. The p16 targets Cdk4 and Cdk6, rather than the CycD, and actually competes with CycD for Cdk binding. Binding of p16 results in changes in conformation of Cdk proteins so that they can no longer bind CycD [29]. The p16 may also deactivate preassembled Cdk4/6_CycD complex blocking their function [29].

The proteins and their complexes are involved in natural degradation. In addition, the CycD protein is also tightly regulated by ubiquitin-dependent degradation [2, 13, 23].

1.2 Related work

Over the past two decades considerable efforts have been directed towards Petri net based investigation of biological systems. A series of biological phenomena modelled and simulated in terms of Hybrid Functional Petri Net (HFPPN) include molecular interactions in the flower developmental network of *Arabidopsis thaliana* [19], lac operon gene regulatory mechanism in the glycolytic pathway of *Escherichia coli* [9], cell fate specification during *Caenorhabditis elegans* vulval development [21], antifolate inhibition of folate metabolism [3], validation of transcriptional activity of the p53 [12], glycolytic pathway controlled by the lac operon gene [11], apoptosis signalling pathway [26], circadian rhythms of *Drosophila* [26], switching mechanism of λ phage [26].

In [16] the authors proposed a hybrid Petri net model of cell cycle. The model comprises both stochastic and deterministic approaches. In this model, stochasticity is used to capture change of the cell size and effect of noises. This model is centered upon interactions between complexes CycB-Cdk1, Cdh1-APC, and monomers Cdc14 and Cdc20 [33]. The study expands macro-level understanding of cell cycle control. However, this study does not provide any insights into understanding quantitative behavior of biological components involved in the cell cycle regulation. Indeed, cell cycle regulation is a complex biological mechanism that consists of hundreds of biological components, processes and pathways. It is hard if not impossible to perform quantitative analysis of cell cycle regulation based on modest size model.

1.3 Contributions

The present research exploits HFPN to create a model of p16-Cdk4/6-Rb pathway, which is a cornerstone of cell cycle regulation at G1/S checkpoint. We combine biological facts described in Subsection 1.1 and quantitative knowledge on reaction rates provided in [11, 12] in a HFPN model. Then we use Cell Illustrator software to perform simulation-based model checking to validate the HFPN model. Simulation-based model checking in general provides interesting biological insights which could be used for future wet-lab experiments [22]. Once the model validated it can be used for obtaining broader understanding of cell cycle regulation.

The manuscript is organized as follows. Section 2 provides a succinct background on HFPN. In Section 3 we develop a HFPN model of p16-Cdk4/6-Rb pathway, and explain relationship between HFPN objects and their biological counterparts. Section 4 presents and analyzes the simulation results. Finally, conclusions are outlined in Section 5.

2 Hybrid Functional Petri Net

Biological systems are characterized by interaction of different structured processes. A continuous process is used to represent a biological reaction, at which a real number called the reaction speed or reaction rate is assigned as a parameter. Concentration change of the biological components or substrates after the biological reaction is completed is also represented as a real number. Promotion/inhibition mechanisms and checking for presence of this or that biological component or phenomenon are typical discrete processes. Change of quantity in a discrete process is usually expressed by integers or Boolean values.

When modelling biological pathways it is desirable to use a modelling framework that combines both continuous and discrete processes. Related software tools are consequently expected to comprise different structured data types including real numbers, integers, Boolean, etc. HFPN [26, 21] was originally proposed for modelling and simulating biological systems employing hybrid structure and dedicated software Cell Illustrator [11, 27] provides suitable platform for visualization and simulation of HFPN models.

While modelling with HFPN, the researchers prefer to use terminology that is slightly different than the traditional one [28]. In order to ensure compliance with the biological content Petri net objects such as place, transition, arc and token are respectively renamed as entity, process, connector and quantity. To increase the readability of the paper below we provide a brief description of HFPN model elements. For more detailed information on this issue the readers are referred to [10].

In context of HFPN an *entity* is an abstract object that represents biological component or substrate such as DNA, mRNA, protein, enzyme, complex of proteins, etc. Each entity is assigned a numeric value called *quantity*, which stands for concentration of related substrate. Variables are used to carry concentration values. A *process* is another abstract object that is used to model

biological reaction or phenomenon like transcription, translation, binding, nuclear export/import, ubiquitination and natural degradation. A process defines the change rate of entity value and establishes interactions among entities. Rate of change is expressed as a formula.

Table 1. Correspondence between biological components and HFPN entities.

Entity name	Entity type	Variable	Initial value	Value type
p16mRNA	Continuous	$m1$	0	Double
p16(C)	Continuous	$m2$	0	Double
p16(N)	Continuous	$m3$	0	Double
CDK4mRNA	Continuous	$m4$	0	Double
CDK4(C)	Continuous	$m5$	0	Double
CDK4(N)	Continuous	$m6$	0	Double
CDK6mRNA	Continuous	$m7$	0	Double
CDK6(C)	Continuous	$m8$	0	Double
CDK6(N)	Continuous	$m9$	0	Double
CycDmRNA	Continuous	$m10$	0	Double
CycD(C)	Continuous	$m11$	0	Double
CycD(N)	Continuous	$m12$	0	Double
CDK4_CDK6	Continuous	$m13$	0	Double
CDK4_CDK6_CycD	Continuous	$m14$	0	Double
Phosphate	Continuous	$m15$	100	Double
RB_DP_E2F	Continuous	$m16$	100	Double
nr_div	Discrete	$m17$	0	Integer
RB_P	Continuous	$m18$	0	Double
DP_E2F	Continuous	$m19$	0	Double
Mutation	Generic	$m20$	true/false	Boolean
p16mutated	Continuous	$m21$	0	Double
G1-dysfunction	Generic	$m22$	true/false	Boolean
p16_CDK4/6(N)	Continuous	$m23$	0	Double
p16_CDK4/6(C)	Continuous	$m24$	0	Double
Ubiquitin	Continuous	$m25$	100	Double
CycD[Ub]	Continuous	$m26$	0	Double
S_phase_genes	Continuous	$m27$	0	Double

The entities and processes are classified as being discrete, continuous and generic. A *discrete entity* is quantified by integers. A *discrete process* causes integer-valued change of a quantity. A *continuous entity* is quantified by real numbers, and consequently *continuous process* causes change of a quantity according to reaction rate formula, which is also represented by real numbers. A *generic entity* contains structured data type composed of different structured data such as Boolean, double and integer. A *generic process* handles structured data assigned to associated entities. In HFPN we distinguish between process connector, inhibitory connector and association connector. A *process connector* is adjacent

from input entity to a process or from process to its output entity. Weight parameter is used to specify an activation threshold. Process connectors ensure flow of tokens in the model. An *inhibitory connector* is used to inhibit a process. Inhibitory connectors are integral elements of biological models with competing processes. An *association connector* establishes adjacency relation between specified entity and process under circumstance that occurrence of related process does not cause concentration change. An association connector is often used in modelling of enzymatic and catalytic reactions.

Table 2. Correspondence between biological phenomena and HFPN processes.

Biological phenomenon	Process	Process type	Process rate
Transcription of p16mRNA	$T1$	Continuous	1
Translation of p16	$T2$	Continuous	$m1*0.1$
Nuclear import of p16	$T3$	Continuous	$m2*0.1$
Transcription of CDK4mRNA	$T4$	Continuous	1
Translation of CDK4	$T5$	Continuous	$m4*0.1$
Nuclear import of CDK4	$T6$	Continuous	$m5*0.1$
Transcription of CDK6mRNA	$T7$	Continuous	1
Translation of CDK6	$T8$	Continuous	$m7*0.1$
Nuclear import of CDK6	$T9$	Continuous	$m8*0.1$
Transcription of CycDmRNA	$T10$	Continuous	1
Translation of CylinD	$T11$	Continuous	$m10*0.1$
Nuclear import of CycD	$T12$	Continuous	$m11*0.1$
Binding of CDK4 and CDK6	$T13$	Continuous	$m6*m9*0.01$
Binding of CDK4.CDK6 and CycD	$T14$	Continuous	$m12*m13*0.01$
Phosphorylation of RB	$T15$	Continuous	$m14*m15*m16*0.1$
Mutation of p16	$T16$	Generic	$m2*0.1$
Binding of p16(N) and CDK4.CDK6	$T17$	Continuous	$m3*m13*0.01$
Nuclear export of p16.CDK4.CDK6	$T18$	Continuous	$m23*0.1$
Ubiquitination of CycD	$T19$	Continuous	$m11*m25*0.01$
Degradation of CycD[Ub]	$T20$	Continuous	$m26*0.5$
Transcription of S phase genes	$T21$	Continuous	$m19*1$

Table 3. Natural degradations in the HFPN model.

Biological phenomenon	Process	Process type	Process rate
Degradation of proteins	$d2, d3, d5, d6, d8, d9, d11 - d18$	Continuous	$mi*0.01$
Degradation of mRNAs	$d1, d4, d7, d10$	Continuous	$mi*0.05$

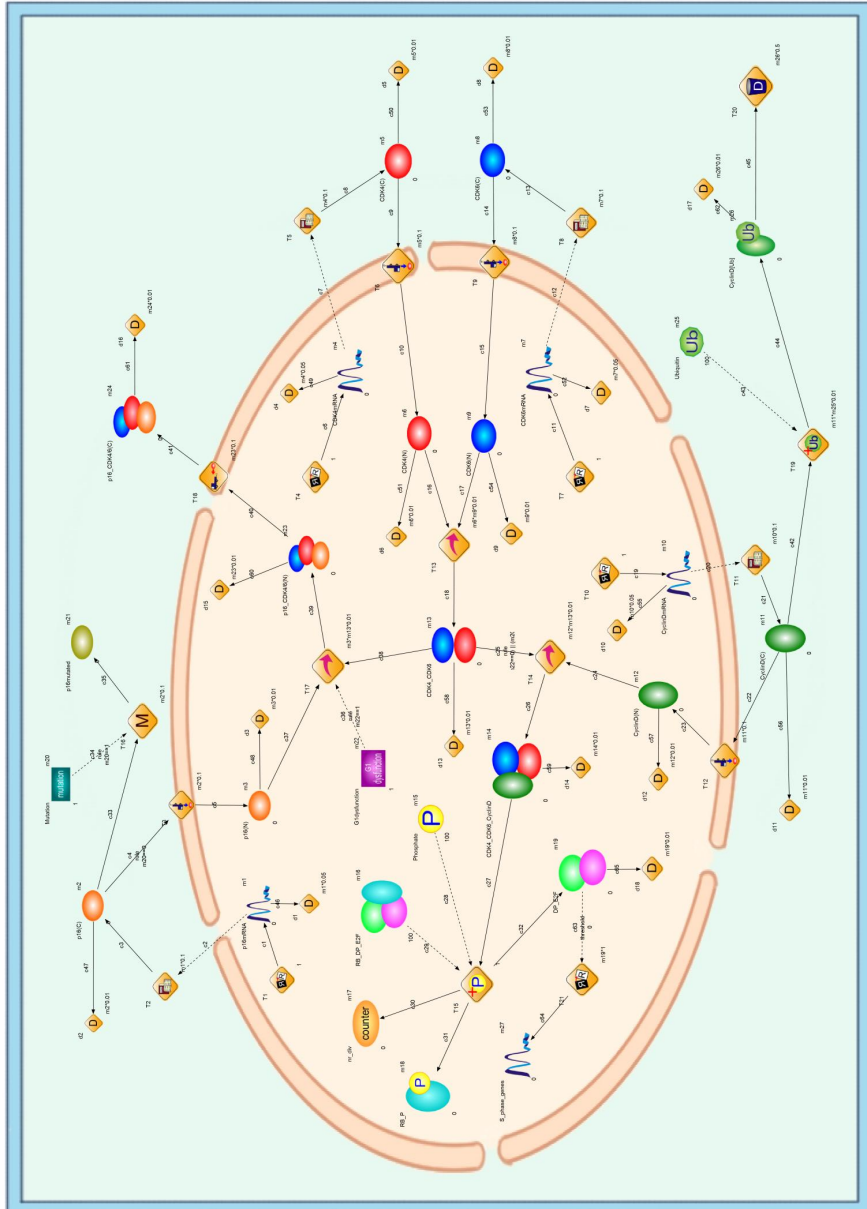
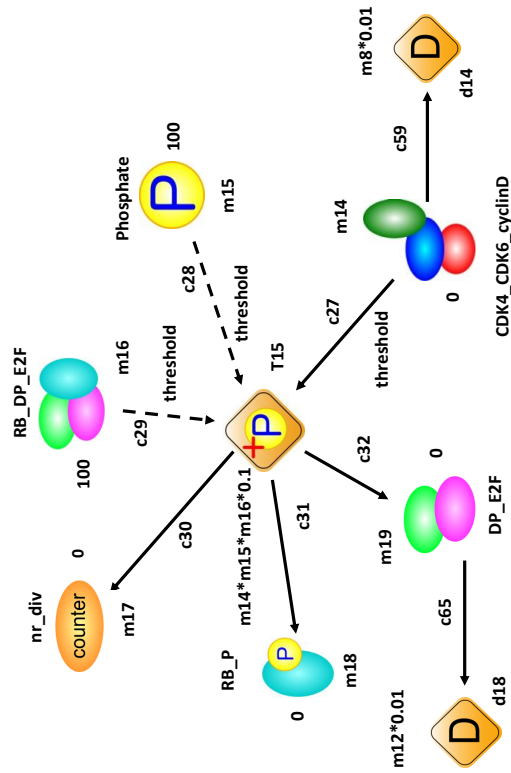


Fig. 1. A Cell Illustrator screen snapshot of p16-CDK4/6-RB HFPN model.



Places			Transitions		
	RB_DP_EZF complex		Phosphate		RB_P phosphorylated protein
	nr_div counter		DP_EZF complex		DP_EZF complex
	CDK4_CDK6_cyclinD complex		CDK4_CDK6_cyclinD		CDK4_CDK6_cyclinD
	D		D		Natural degradation

Fig. 2. A Petri net fragment illustrating phosphorylation of RB and natural degradation of the components involved into the process.

Table 4. Connectors in the HFPN model.

Connector	Firing style	Firing script	Connector type
c4	Rule	m20==1	Input process
c25	Rule	(m20==0 && m22==0) (m20==1 && m22==0) (m20==1 && m22==1)	Input process
c34	Rule	m22==1	Input association
c36	Rule	m20==0	Input process
c2,c7,c12,c20,c28,c29 c43,c63	threshold	0	Input association
c9,c14,c16,c17,c22,c24 c25,c27,c33,c37,c38,c40 c42,c45-c62,c65	threshold	0	Input process
c1,c3,c5,c6,c8,c10 c11,c13,c15,c18,c19,c21 c23,c26,c30,c31,c32,c35 c39,c41,c44,c64	threshold	0	Output process

3 Model Development

In this section we provide step-by-step explanation on how HFPN model of p16-Cdk4/6-Rb pathway is created according to the biological facts provided in Subsection 1.1, and describe relationship between HFPN objects and their biological counterparts.

The entities used in the model are detailed in Table 1. The entities represent mRNAs, nuclear and cytoplasmic proteins, protein complexes, phosphate, ubiquitin, mutation and G1-dysfunction. A variable associated with a continuous entity quantifies concentration of specified substrate. To ensure continual phosphorylation of **Rb** we assume that there exist sufficient amount of phosphate and **Rb_DP_E2F** concentration. This is why variables **m15** and **m16** are initially set to 100. Likewise, **m25** is set to 100 to guarantee continual ubiquitination of **CycD**. The initial concentration of mRNAs and consequently protein monomers and their complexes are set to 0 since simulation starts with transcription of related mRNAs. The entities **G1-dysfunction** and **mutation** are used to indicate boolean status or presence/absence of corresponding events. The entity **nr_div** counts the number of cell divisions.

The processes used in the present research include transcription, translation, nuclear import/export, binding, ubiquitination, phosphorylation and natural degradation. Relationship between processes and biological phenomena are illustrated in Table 2 and Table 3. It was reported that mutations in the p16 binding site result in diminished capability of p16 binding to Cdk4/6. This particularly leads to loss of function of p16 as an inhibitor of Cdk4/6-CycD complex. In this model, boolean status of mutation is controlled by **T16** and **m20**. Assignment **m20==1** constitutes presence of mutation, consequently leading to

occurrence of **T16** which in deed arrests p16 in cytoplasm. Otherwise **T3** occurs generating nuclear import of p16. Likewise, the presence/absence of dysfunction in the G1 phase is controlled by entity **G1-dysfunction** and variable **m22**. Assignment **m22==1** indicates the presence of dysfunction in the G1 phase. Next p16 acts as inhibitor of Cdk4/6-CycD complex. We use two Boolean variables with total of four distinct combinations. The rules set for associated connectors and processes depend on four distinct combinations of two Boolean variables **m20**, which represents the mutation in p16, and **m22**, which stands for the dysfunction in G1 phase. Occurrence of transitions **T3**, **T14**, **T16**, and **T17** respectively depend on the rules on connectors **c4**, **c25**, **c34**, and **c36**. For instance, **T3**, nuclear import of p16, occurs if there is no mutation in p16. That is, **T3** can fire only if **m20==0**. All connectors together with their firing styles, firing scripts, and connector types are described in Table 4. A snapshot of HFPN model is illustrated in Fig. 1.

A net fragment bound to **T15** is shown in Fig. 2. This fragment reveals the structural basis for phosphorylation of Rb. Other than connector rules, the phosphorylation of Rb (**T15**) has its activity rule as: $(m20==0 \ \&\& \ m22==0 \ || \ (m20==1 \ \&\& \ m22==0) \ || \ (m20==1 \ \&\& \ m22==1))$. Here, the first statement part is for the case when p16 is not mutated, and there is no dysfunction in the G1 phase. It is known that replicative senescence should occur if there is no mutation and dysfunction in a cell, which means that the cell stops dividing after 50 divisions [17]. In our model, the **m17** is defined as a counter which keeps track the number of divisions, and in the case of no mutation and no dysfunction, it is checked whether the counter is less than 50 or not. If it is not, the cell should stop dividing, which means that RB should not be phosphorylated after 50 divisions. The other two statement parts in the activity rule of **T15** are the cases when p16 is mutated. If p16 is mutated, then the replicative senescence will not occur and the cell will divide continually leading to progression of malignancy.

Process rates are chosen in accordance with the reaction speeds for specific reaction types adopted in [11, 12]. Process rate for transcription is set to 1 to ensure continual mRNA production. The process rates are listed in Table 2.

4 Simulations and Results

In this research, simulations were carried out using Cell Illustrator 5.0 (professional version) that is licensed to Eastern Mediterranean University. Simulation results for concentration behaviour of nuclear and cytoplasmic proteins and their complexes are illustrated in Fig. 3-5. We performed simulations for the following four cases:

1. The p16 is not mutated and there is no dysfunction in the G1 phase ($m20==0 \ \&\& \ m22==0$).
2. The p16 is not mutated and there is dysfunction in the G1 phase ($m20==0 \ \&\& \ m22==1$).
3. The p16 is mutated and there is no dysfunction in the G1 phase ($m20==1 \ \&\& \ m22==0$).

4. The p16 is mutated and there is dysfunction in the G1 phase ($m20==1$ && $m22==1$).

It is generally assumed that p16 is transported to the nucleus and acts as a CKI to regulate the G1/S cell cycle checkpoint. This phenomenon has been reported in normal cells where the protein was mainly found in the nucleus but not in the cytoplasm [5]. This fact is supported by the simulation results that are illustrated in Fig.3. For all four cases the concentration of p16(C) is at level 17.5 after almost 50 pt (Petri net time), at which the steady state starts. On the other hand, if there is no dysfunction in the G1 phase ($m22==0$) and if p16 is not mutated ($m20==0$) p16(N) is at level 175, that is, almost 10 times more than that of in cytoplasm. It should be noticed that small oscillations in the p16(C) graphs are result of natural degradation which is 10 times slower than the translation process. Mutation in p16 arrests it in cytoplasm. This is why when p16 is mutated its concentration in nucleus is constantly 0.

Healthy and functioning p16 protein forms a complex with Cdk4/6 if it detects a dysfunction. Simulation results, that are illustrated in Fig. 3 and Fig. 4, have shown that p16-Cdk4/6 concentration in cytoplasm and nucleus are respectively at level 125 and 15, i.e. p16-Cdk4/6 concentration in cytoplasm is almost 8 times more than that in nucleus, indicating that p16-Cdk4/6 is accumulated in cytoplasm rather than in nucleus. We were not able to find an experimental result to compare this finding with. The reasonable explanation for this fact however could be the difference between reaction rates of nuclear export and binding, i.e., the former is 10 times faster than the latter.

It was reported in [24] that levels of Cdk proteins in cells vary little throughout the cell cycle. Simulation results for change of Cdk4 and Cdk6 concentrations in nucleus and cytoplasm are shown in Fig. 4-5. These results fully agree with this fact, in sense that concentration of Cdk4 and Cdk6 in nucleus and cytoplasm are respectively at the level 12 and 17 throughout the simulations. This fact remains true even for Cdk4/6 (Fig. 5).

5 Conclusions

The present research explores interaction between HFPN and biological processes, to the benefit of both fields. On the one hand we adopt HFPN for modelling and simulation of specific biological pathways, and consequently expand the list of HFPN applications. On the other hand, through modelling and simulating with HFPN we obtain broader understanding of cell cycle regulation.

The fact that in normal cells p16 protein is mainly accumulated in the nucleus but not in the cytoplasm [5] is confirmed by simulation results. The simulation results have shown that the p16-CDK4/6 protein complex is accumulated in cytoplasm rather than in nucleus. We were not able to find an experimental result to compare this finding with. The simulation results are in agreement with the fact that levels of Cdk proteins in cells vary little throughout the cell cycle [24].

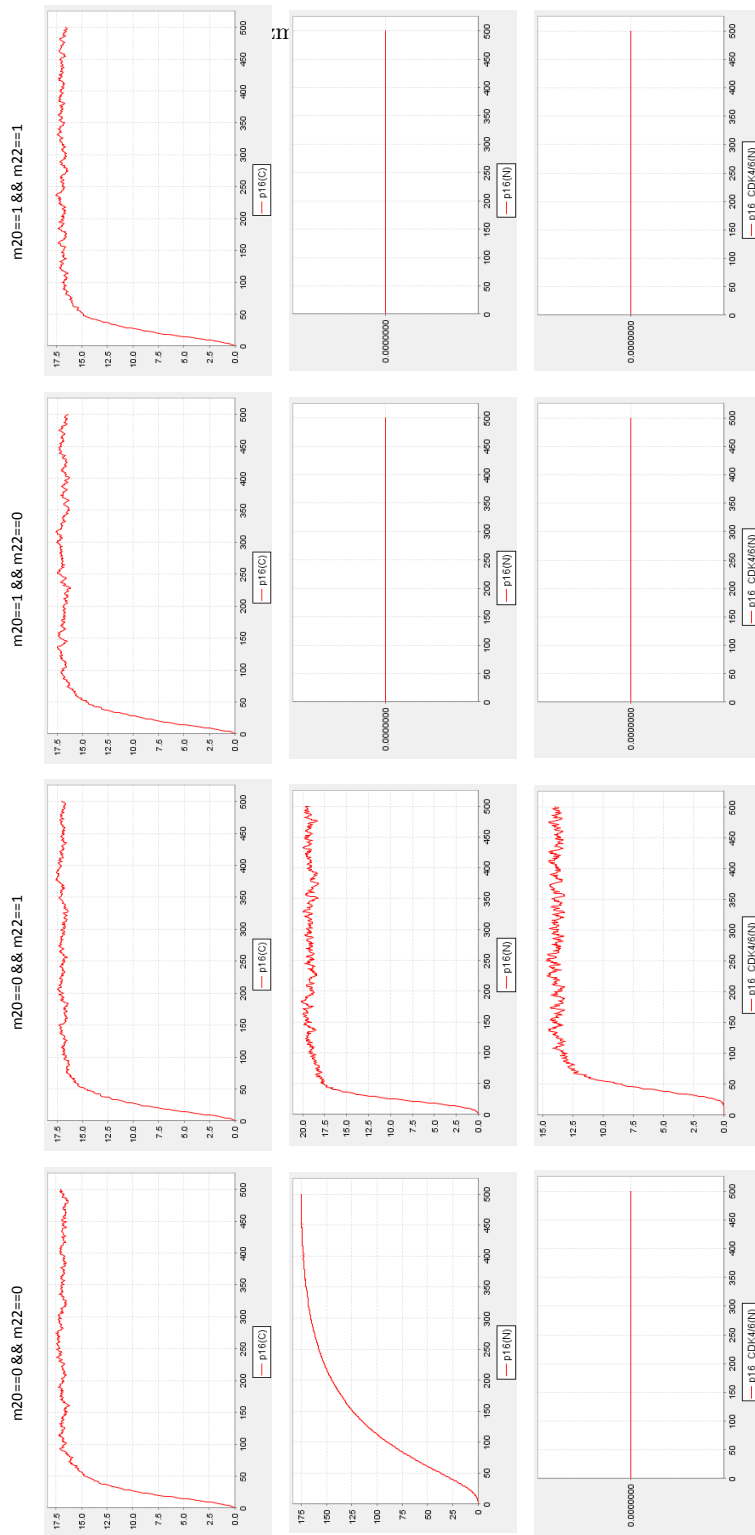


Fig. 3. Simulation results for $p16(C)$, $p16(N)$ and $p16_CDK4/6$.

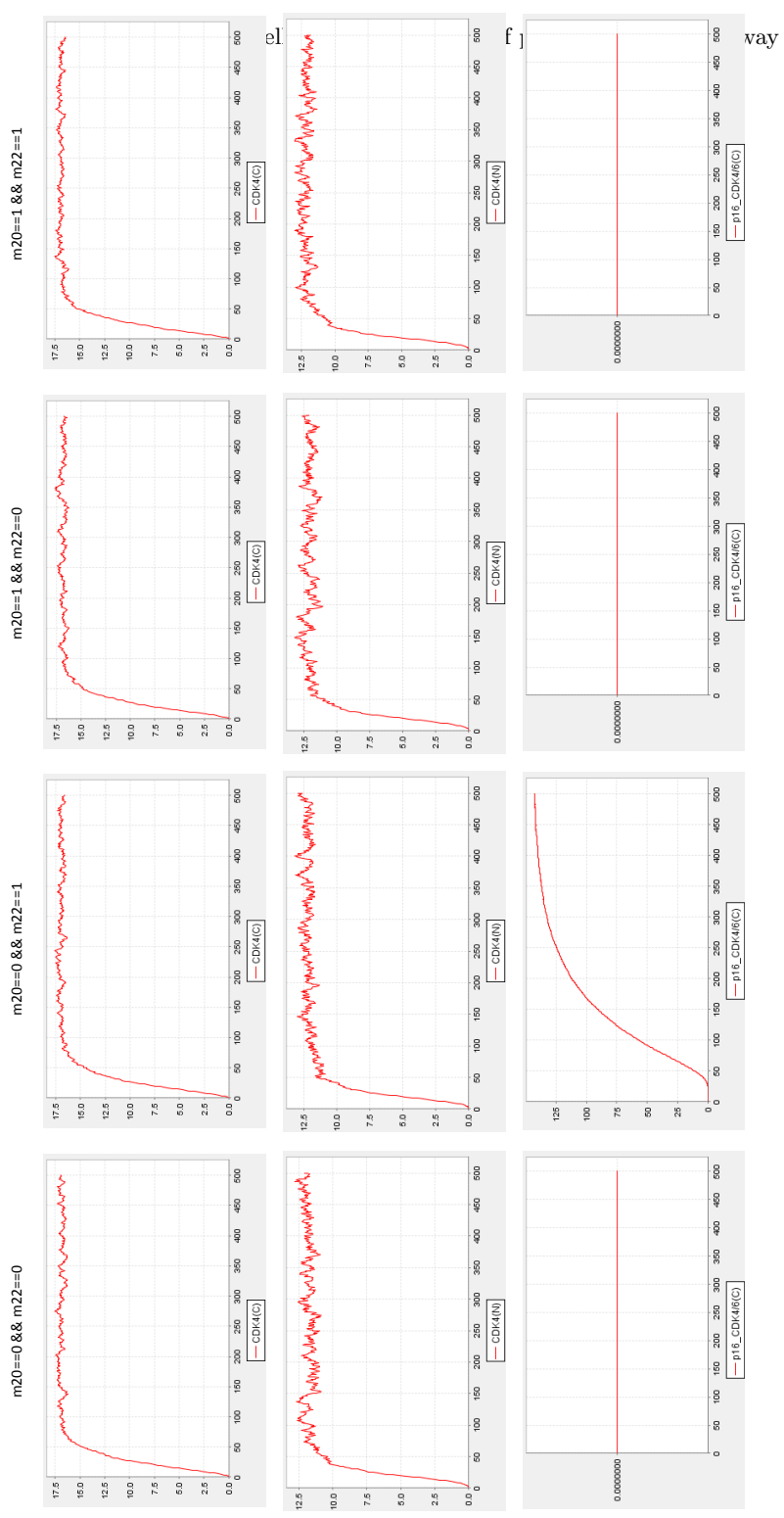


Fig. 4. Simulation results for CDK4(C) and CDK4(N).

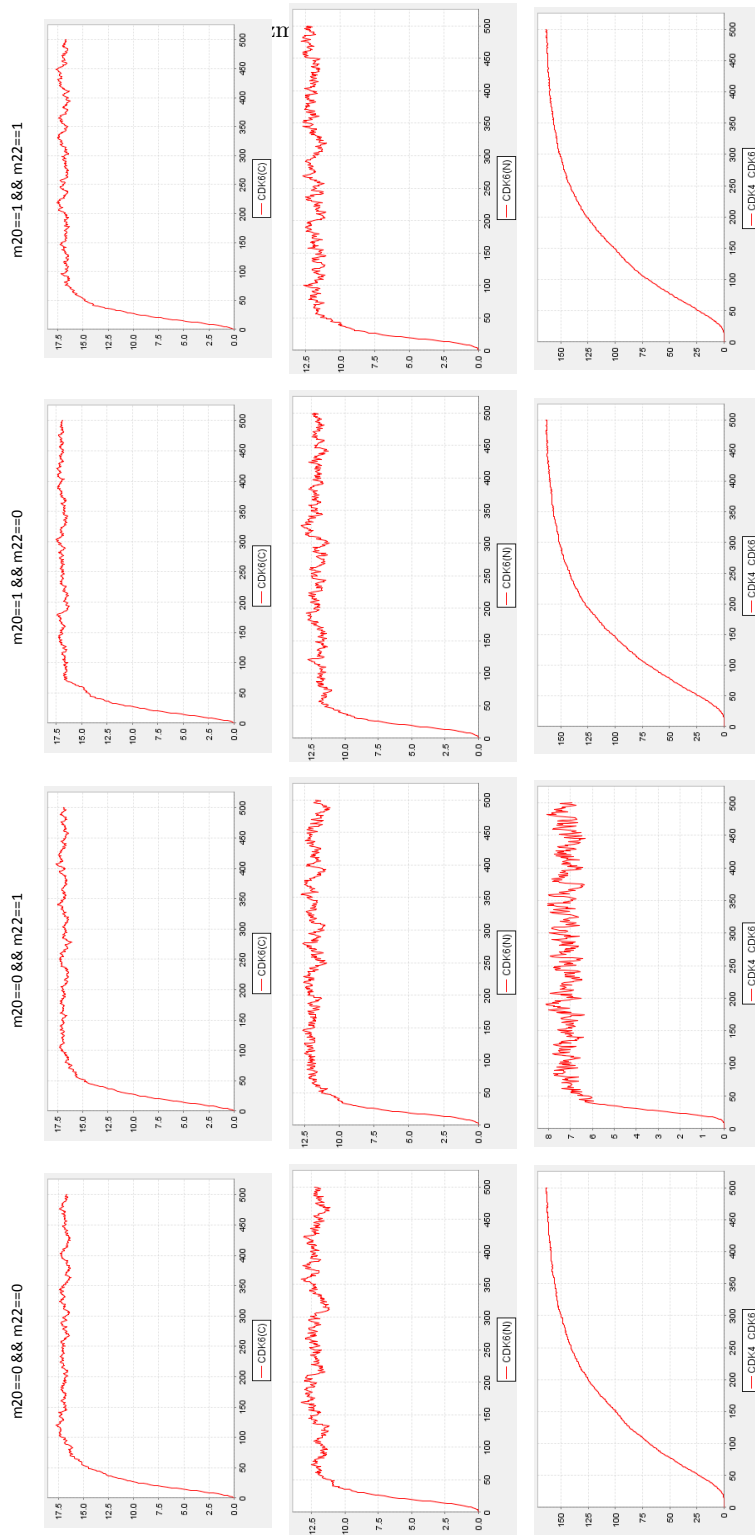


Fig. 5. Simulation results for CDK6(C), CDK6(N) and CDK4/6.

References

1. Agherbi, H., Gaussmann-Wenger, A., Verthuy, C., Chasson, L., Serrano, M., Djabali, M.: Polycomb mediated epigenetic silencing and replication timing at the INK4a/ARF locus during senescence. *PLoS One* **4**(5), e5622 (2009).
2. Alao, J.P.: The regulation of cyclin D1 degradation: roles in cancer development and the potential for therapeutic invention. *Molecular Cancer* **6**(24) (2007).
3. Assaraf, Y. G., Ifergana, I., Kadryb, W. N., PinteRb R. Y.: Computer modelling of antifolate inhibition of folate metabolism using hybrid functional petri nets. *Journal of Theoretical Biology* **240**, 637-647 (2006).
4. Baker, D.J., Perez-Terzic, C., Jin, F., Pitel, K., Niederlander, N.J., Jeganathan, K., Yamada, S., Reyes, S., Rowe, L., Hiddinga, H.J., Eberhardt, N.L., Terzic, A., van Deursen, J.M.: Opposing roles for p16Ink4a and p19Arf in senescence and ageing caused by BubR1 insufficiency. *Nat Cell Biol* **10**(7), 825-836 (2008).
5. Bartkova, J., Lukas, J., Guldborg, P., Alsnér, J., Kirkin, A.F., Zeuthen, J., Bartek, J.: The p16-cyclin D/Cdk4-pRb pathway as a functional unit frequently altered in melanoma pathogenesis. *Cancer Res*, **56**(23), 5475-5483 (1996).
6. Batt, G., Ropers, D., de Jong, H., Geiselman, J., Mateescu, R., Page, M., Schneider, D.: Validation of qualitative models of genetic regulatory networks by model checking: analysis of the nutritional stress response in *Escherichia coli*. *Bioinformatics* **21**(Suppl 1) 19-28 (2005).
7. Calder, M., Vyshemirsky, V., Gilbert, D., Orton, R.: Analysis of signalling pathways using the prism model checker. In: *Proceeding of Computational Methods in Systems Biology*, 3-5 April, Edinburgh, pp.179-190 (2005).
8. Campisi, J.: Cellular senescence as a tumorsuppressor mechanism. *Trends Cell Biol* **10**, S27-S31 (2001).
9. Castellini, A., Franco, G., Manca, V.: Hybrid functional Petri nets as MP systems. *Nat Comput* **9**(1), 61-81 (2010).
10. Cell IllustratorTM: User Guide. The University of Tokyo, 2002-2010 Human Genome Center, Institute of Medical Science.
11. Doi, A., Fujita, S., Matsuno, H., Nagasaki, M., Miyano, S.: Constructing biological pathway models with Hybrid Functional Petri Nets. *In Silico Biol* **4**(3), 271-291 (2004).
12. Doi, A., Nagasaki, M., Matsuno, H., Miyano, S.: Simulation-based validation of the p53 transcriptional activity with hybrid functional Petri net. *In Silico Biology* **6**(1-2), 1-13 (2006).
13. Germain, D., Russell, A., Thompson, A., Hendley, J.: Ubiquitination of free cyclin D1 is independent of phosphorylation on threonine 286. *J Biol Chem* **275**(16), 12074-12079 (2000).
14. Enoch, T., Nurse, P.: Coupling M phase and S phase: controls maintaining the dependence of mitosis on chromosome replication. *Cell* **65**(6), 921-923 (1991).
15. Fisher, J., Piterman, N., Hajnal, A., Henzinger, T.A.: Predictive modeling of signaling crosstalk during *C. elegans* vulval development. *PLoS Comput Biol* **3**(5), e92 (2007).
16. Herajy, M., Schwarick, M.: A hybrid Petri net model of the eukaryotic cell cycle. In: *Proc. 3th International Workshop on Biological Processes and Petri Nets*, 29-43, 2012.
17. Hayflick, L.: The Limited in Vitro Lifetime of Human Diploid Cell Strains. *Exp Cell Res* **37**, 614-636 (1965).

18. Heath, J., Kwiatkowska, M., Norman, G., Parker, D., Tymchyshyn, O.: Probabilistic model checking of complex biological pathways. *Theor Comput Sci* **391**(3), 239-257 (2008).
19. Kaufmann, K., Nagasaki, M., Jauregui, R.: Modelling the molecular interactions in the flower developmental network of *Arabidopsis thaliana*. *Annals of Botany* **107**(9), 1545-1556 (2011).
20. Kwiatkowska, M.Z., Norman, G., Parker, D.: Using probabilistic model checking in systems biology. *SIGMETRICS Performance Evaluation Review*, **35**(4), 14-21 (2008).
21. Li, C., Nagasaki, M., Ueno, K., Miyano, S.: Simulation-based model checking approach to cell fate specification during *Caenorhabditis elegans* vulval development by hybrid functional Petri net with extension. *BMC Systems Biology* **3**(42) (2009).
22. Li, C., Nagasaki, M., Koh, C.H., Miyano, S.: Online model checking approach based parameter estimation to a neuronal fate decision simulation model in *Caenorhabditis elegans* with hybrid functional Petri net with extension. *Mol Biosyst.* **7**(5), 1576-1592, (2011).
23. Lin, D.I., Barbash, O., Kumar, K.G., Weber, J.D., Harper, J.W., Klein-Szanto, A.J., Rustgi, A., Fuchs, S.Y., Diehl, J.A.: Phosphorylation-dependent ubiquitination of cyclin D1 by the SCF(FBX4-alphaB crystallin) complex. *Mol Cell* **24**(3), 355-366 (2006).
24. Malumbres, M., Barbacid, M.: Cell cycle, CDKs and cancer: a changing paradigm. *Nat Rev Cancer*, **9**(3), 153-166 (2009).
25. Matheu, A., Maraver, A., Collado, M., Garcia-Cao, I., Canamero, M., Borras, C., Flores, J.M., Klatt, P., Vina, J., Serrano, M., Anti-aging activity of the Ink4/Arf locus. *Aging Cell* **8**(2), 152-161 (2009).
26. Matsuno, H., Tanaka, Y., Aoshima, H., Doi, A., Matsui, M., Miyano, S.: Biopathways representation and simulation on Hybrid Functional Petri Nets. *In Silico Biol* **3**(3), 389-404 (2003).
27. Nagasaki, M., Doi, A., Matsuno, H., Miyano, S.: Genomic object net: I. A platform for modelling and simulating biopathways. *Appl Bioinformatics* **2**(3), 181-184 (2004).
28. Reisig, W.: *Petri Nets: an introduction*. EATCS, Monographs on Theoretical Computer Science. Springer, New York, 1985.
29. Russo A.A., Tong, L., Lee, J.O., Jeffrey, P.D., Pavletich, N.P.: Structural basis for inhibition of the cyclin-dependent kinase Cdk6 by the tumour suppressor p16INK4a. *Nature* **395**(6699), 237-243 (1998).
30. Sherr C.J.: Cancer cell cycle. *Science* **274**, 1672-1677 (1996).
31. Stevaux O., Dyson N.J.: A revised picture of the E2F transcriptional network and RB function. *Curr Opin Cell Biol* **14**, 684-691 (2002).
32. Trimarchi J.M., Lees J.A.: Sibling rivalry in the E2F family. *Nat Rev Mol Cell Biol* **3**, 11-20 (2002).
33. Tyson, J., Novak, B.: *A Systems Biology View of the Cell Cycle Control Mechanisms*. Elsevier, San Diego, CA, (2011).
34. Vidal A., Koff A.: Cell-cycle inhibitors: three families united by a common cause. *Gene* **247**(1-2), 1-15 (2000).
35. Walkley, C.R., Orkin, S.H.: RB is dispensable for self-renewal and multilineage differentiation of adult hematopoietic stem cells. *Proc Natl Acad Sci USA*, **103**(24), 9057-9062 (2006).
36. Weinberg, R.A., The retinoblastoma protein and cell cycle control. *Cell* **81**(3), 323-330 (1995).